BJR

https://doi.org/10.1259/bjr.20170868

Received: 15 November 2017 | Revised: 05 September 2018 | Accepted: 23 September 2018

Cite this article as:
De Rubeis G, Galea N, Ceravolo I, Dacquino GM, Carbone I, Catalano C, et al. Aortic valvular imaging with cardiovascular magnetic resonance: seeking for comprehensiveness. *Br J Radiol* 2018; **91**: 20170868.

REVIEW ARTICLE

Aortic valvular imaging with cardiovascular magnetic resonance: seeking for comprehensiveness

GIANLUCA DE RUBEIS, MD, NICOLA GALEA, MD, PhD, ISABELLA CERAVOLO, MD, GIAN MARCO DACQUINO, MD, IACOPO CARBONE, MD, CARLO CATALANO, MD and MARCO FRANCONE, MD, PhD

Department of Radiological, Oncological and Pathological Sciences,"Sapienza" University of Rome, Rome, Italy

Address correspondence to: ProfMarcoFrancone
E-mail: *marco.francone@uniroma1.it*

The authors Gianluca De Rubeis and Nicola Galea contributed equally to the work.

ABSTRACT

Cardiovascular magnetic resonance (CMR) has an emerging role in aortic valve disease evaluation, becoming an all-in-one technique. CMR evaluation of the anatomy and flow through the aortic valve has a higher reproducibility than echocardiography. Its unique ability of *in vivo* myocardial tissue characterization, significantly improves the risk stratification and management of patients. In addition, CMR is equivalent to cardiac CT angiography for trans-aortic valvular implantation and surgical aortic valve replacement planning; on the other hand, its role in the evaluation of ventricular function improving and post-treatment complications is undisputed. This review encompasses the existing literature regarding the role of CMR in aortic valve disease, exploring all the aspects of the disease, from diagnosis to prognosis.

INTRODUCTION

Aortic valvular disease (AVD) affects overall 0.9% of the general population.[1] There is an increasing prevalence among the elderly (*i.e.* >65 years), which reflects the age-related progressive development of leaflet sclerosis and calcium deposition, leading to valvular remodelling.[2]

Crucial to patient management is the correct grading of disease severity, which depends on multiple factors such as the anatomy of the leaflets, valve hemodynamics and left ventricular (LV) function, in addition to patient symptoms. Particularly, in asymptomatic patients, imaging plays an important role in the initial evaluation of aortic valve disease.

Since the optimal medical therapy is only able to slow disease progression or reduce its hemodynamic effects on LV function, to establish the appropriate time for surgical treatment is fundamental.[3]

According to guidelines on management of aortic stenosis, surgical valve replacement is recommended in symptomatic patients with severe disease, and in asymptomatic patients with severe disease associated with LV impairment or while undergoing to cardiac surgery for other reasons.[4,5] However, minimally invasive percutaneous interventional techniques, like transcatheter aortic valve implantation (TAVI), have been recently established as a valid option in individuals with a high or prohibitive surgical risk and, the results of ongoing studies, such as SURTAVI[6] and PARTNER 2[7] trials, could potentially extend the indications for TAVI to patients with intermediate risk.

In this complex clinical scenario, although echocardiography remains the primary imaging modality both for both initial assessment and longitudinal evaluation of AVD,[4,5,8,9] Cardiovascular magnetic resonance (CMR) is being increasingly used in daily clinical practise due to its versatility, which allows a comprehensive evaluation of the different aspects of valvular disease[4,5,8]

CMR is a viable and robust alternative for AVD assessment in patients with poor echo-windows evaluation or when the discrepancy between the clinical features and results on two-dimensional (2D) echocardiogram and Doppler ultrasound results makes the decision making difficult.[4,5] Furthermore, CMR can assess the consequences of the valvular lesions on ventricular remodelling by combining the assessment of LV function and myocardial fibrosis.[5,9–13]

The aim of this review is to provide a comprehensive and updated overview of CMR potentials in aortic AVD, from

disease staging and pre-procedural selection of candidates to surgical replacement to the evaluation of post-operative complications.

Well-known information regarding stenotic/insufficient/mixed AVDs imaging is integrated with new emerging clinical applications of the technique, like the evaluation of patients with bicuspid aortic valves or the pre-TAVI screening. Finally, the prognostic implications related to the presence of myocardial fibrosis will be analysed, with CMR providing a unique imaging-based "histology *in vivo*".

Normal anatomy, variants and related clinical implications

The aortic valve (AV) is a trifoliate structure supported by a fibrous skeleton, linked with the anterior leaflet of the mitral valve. The three valve leaflets (left, right and non-coronary), or cusps, are thin and symmetric flaps of fibrous tissue that open uniformly, pushing into their respective sinuses of Valsalva (SV) during systole. The aortic root is a complex structure, schematically outlined with three parallel virtual rings (sino-tubular junction, ventricular-arterial junction and basal attachment of AV leaflets) and one crown shaped line with three contour bumps (representing the aortic bulb with SV).[14] Each cusp is anchored to the aortic wall by the outward semicircular edges. The double free edge is suspended within the aortic lumen during the systole, whereas it is pushed back by retrograde aortic flow. Vortices generated in the SV during diastole play a role in the valve mechanics by relieving abnormal stress on aortic leaflets and facilitating smooth valve closure.[15] The joining points between the valve cusp attachments and the annulus are called commissures.

The normal tricuspid morphology is easily recognized by the so-called "Mercedes sign" (three-pointed star) on cineMR images obtained on axial planes passing through the aortic bulb.

Echocardiography is generally sufficient to assess AV morphology; however, in the case of poor acoustic window or unclear morphology, CMR is indicated to provide a detailed assessment of valve and root anatomy.[4]

The most common anatomical abnormalities of the AV are the numeric variants of the leaflets and the fusion of the commissures (Figure 1).

The unicuspid variant is rare (0.02% of general population) and is frequently associated with early severe aortic stenosis occurring in infancy or childhood and with ascending aortic dilatation.[16] Unicuspid AV may be classified into a unicommissural form, which has an eccentric loophole-shaped orifice, and an acommissural form with a central orifice similar to a diaphragm.[17]

Biscuspid aortic valve (BAV) is the most common congenital heart disease (1–2% of the population, familial in 9% of cases)[18] and is increasingly recognized as a complex and heterogeneous clinical entity; it is frequently associated with other congenital cardiovascular abnormalities (coartaction, supra- or subvalvar aortic stenosis, ventricular septal defect) or genetics disorders, such as Marfan's syndrome and Turner syndrome.[18,19] BAV is commonly complicated by valvular stenosis (51% of cases), aortic regurgitation (17%) or mixed lesions (9%).[20] BAV may be characterized by two specular leaflets with two SV or it can result from the congenital fusion of two leaflets. The most common type is due to the fusion of the right and left coronary leaflets

Figure 1. Normal aortic valve and congenital variants. Comparison between "on valve plane" cine-MR images and schemes of valve anatomy (bottom). A normal tricuspid aortic valve (A, B), unicuspid unicommissural valve (C, D), bicuspid valve due to the congenital fusion of right coronary and non-coronary cusps (E, F) and a quadricuspid valve with incomplete closure of the valvular orifice during diastolic phase (G, H) are shown. (G, Courtesy of Prof Guido Ligabue).

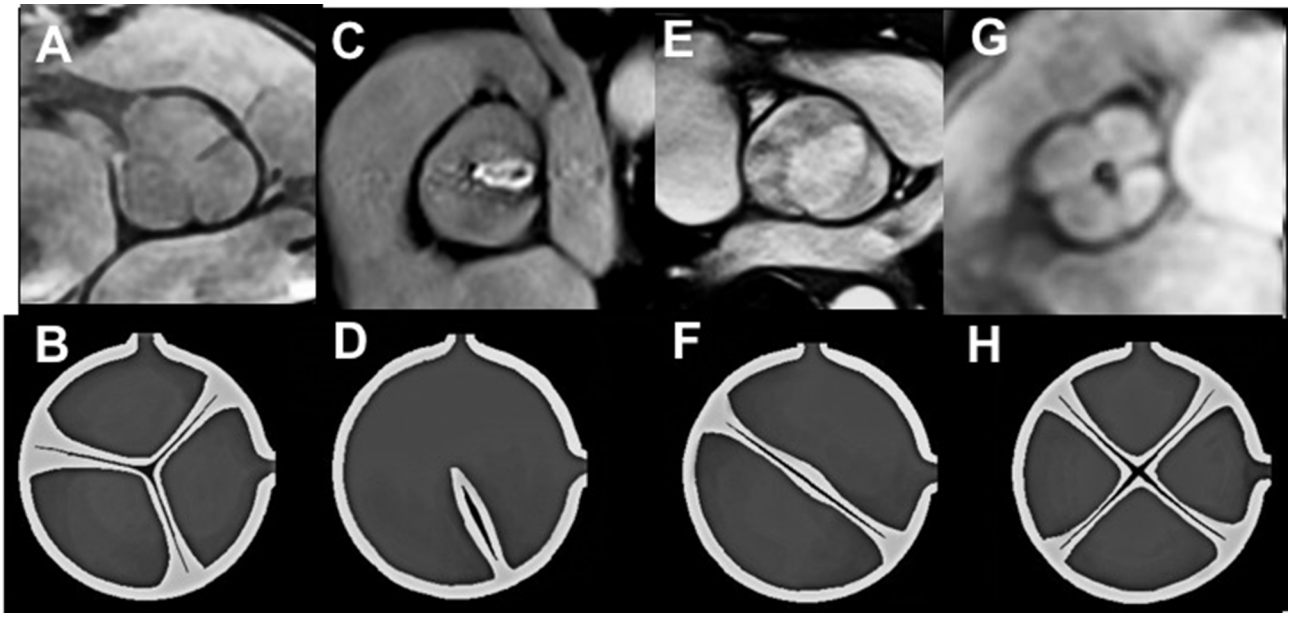

(RL-BAV type, 60% of cases), followed in prevalence by the fusion between the non-coronary and right coronary cusps with a right-left leaflet orientation (12% of cases).[21]

Dilatation of SV or ascending aorta is frequently reported in patients with BAV, with a prevalence ranging from 20 to 84%.[22] Serial evaluation of the size and morphology of the aortic sinuses and ascending aorta is recommended in patients with a bicuspid aortic valve and an aortic diameter greater than 4.0 cm, with the examination interval determined by the degree and rate of progression of the aortic dilatation, and by family history.[4]

A well-established association between BAV phenotype and an aortic enlargement independent of valve function has been extensively demonstrated [23] and there has been growing interest in exploring the relationships between specific anatomy, downstream flow pattern and pathophysiology of aortic dilatation by using the novel four-dimensional (4D) flow CMRI.[24] The altered valve opening confers the typical "fish mouthed" appearance to the valve opening and modifies the aortic hemodynamics, by distorting the LV outflow, with an eccentric jet directed towards the mid-ascending aortic wall, resulting in an increased localized wall shear stress.[24]

Nowadays, the only considered quantitative criterion predicting aortic dissection in BAV is the diameter and the 2017 AHA/ACC report on Appropriate Use Criteria for Multimodality Imaging recommend a close surveillance (<1 year, including CMR) in patients with BAV and aortic diameters greater than 4.5 or 4.0 cm with a rapid rate of aortic diameter change [or] family history of aortic dissection.[5]

It is still controversial, if specific BAV phenotypes are more associated with aneurysmal dilatation and increased risk of aortic dissection 23 , and long-term risk prediction, based on different phenotypes of BAV, could be of great benefit in tailoring individual follow-up programme or preventive management in the future.

Quadricuspid aortic valves are extremely rare variants (0.01% at autopsy), generally associated with abnormal valve function (84% of cases, 75% of which have aortic regurgitation).[25]

AORTIC VALVE PATHOLOGY

Aortic valve stenosis

Aortic stenosis (AS) is defined as the obstruction of the left ventricular outflow tract (LVOT) caused by valve disease.[26] The prevalence of AS in the population aged 65 years or older is approximately 2–9% and the survival rate, without repair, is 50% at 10 years.[27,28] According to the AHA/ACC classification, the severity of aortic stenosis can be divided into four stages: A (at risk of AS), B (progressive AS), C (asymptomatic, severe AS) and D (symptomatic, severe AS).[4] Each of these stages is based on valve anatomy (planimetry), valve hemodynamics, hemodynamic consequences on the LV and symptoms. Clinical grading of AS is currently performed non-invasively by Doppler transthoracic echocardiography through measurement of the aortic peak velocity (Vpeak), mean transaortic pressure gradient, and the effective aortic valve area (AVA).

Severe AS is defined as peak velocity higher than 4.0 m s^{-1}, corresponding to a mean aortic valve gradient of 40 mmHg. Although AVA is not strictly included in the definition, an area <1.0 cm^2 is considered pathological.[2,4]

Valve planimetry can be assessed by different techniques with various approaches, including TTE (indirectly through continuity equation), transesophageal echocardiography (TEE) and CT angiography (CTA) (direct planimetry), and invasive coronary angiography (ICA) (Gorlin formula).

Nevertheless, all of them present some drawbacks, such as poor acoustic windows (TTE, TEE), invasiveness (ICA), radiation exposure (ICA, CTA) and an indirect measurement (TTE and ICA).[29]

CMR evaluation is indicated mainly in cases of inappropriate acoustic windows, which occurs in up to 30% of cases,[30] and complex valve anatomy.[4,5] Two methods have been described for AVA measurement with CMR; direct planimetry and the continuity equation with good agreement between these two methods (correlation: R2 = 0.86, $p < 0.0001$).[31]

Direct planimetry is performed by manually tracing the internal leaflet borders on CineMR images in the aortic valve plane during the opening peak,[32] which is operator-dependent and hence prone to measurement errors in severe or heavily calcified valves, because of the low signal of calcifications and turbulences close to the leaflet borders, and irregularity of the stenotic orifice shape. Continuity equation method offers an indirect AVA estimation, based on the principle of conservation of the mass, which uses the quantitative analysis of the transvalvular aortic flows through phase contrast sequences (PC-MRI) acquired in the valve plane (AVA = stroke vol/velocity–time integral at the aortic flow velocity peak).[33]

Multimodality comparisons showed no differences between AVA measurements obtained by CMR versus 2D TTE, three-dimensional (3D) TTE, Doppler echocardiography, TEE and ICA[29,34,35] whereas both 2D TTE and ICA underestimated valve annulus dimensions compared to CMR ($p < 0.01$).[29] Moreover, the sensitivity and specificity of CMR to detect AVA ≤0.80 cm^2, compared with catheterization, were 78 and 89%, which are higher than TEE (70 and 70%) and TTE (74 and 67%),[34] respectively.

The degree of valve stenosis can be evaluated by two techniques: direct visualization of the jet (qualitative) and PC-MRI (quantitative).[36] The qualitative method is performed by observing the flow void artifact seen as a jet in the aortic root during systole on cineMR images, caused by the acceleration of blood flow through the valve orifice on LVOT view[36] (Figure 2).

CineMR imaging is also crucial to determine the geometry/direction of the jet and the exact location where the flow acceleration artifact originates, which may differentiate between valvular and

Figure 2. CMR (top) and CCTA (bottom) from a 74-year-old female with severe calcified aortic stenosis. On cine-MR "on-valve plane" and three-chamber views acquired in systolic phase (A, B) valve calcifications appear as hypointense thicknening of the luminal edge of the cusps (A, arrow); severe stenosis is demonstrated by markedly reduced opening of the valve orifice (A) and systolic jet on downstream aortic flow on three chamber view (B, arrow). The corresponding CCTA images show diffuse valvular calcifications (black arrow) on multiplanar reformatted "valve plane" (C) and three-chamber images(D) CCTA, coronary CT angiography; CMR, cardiovascular magnetic resonance.

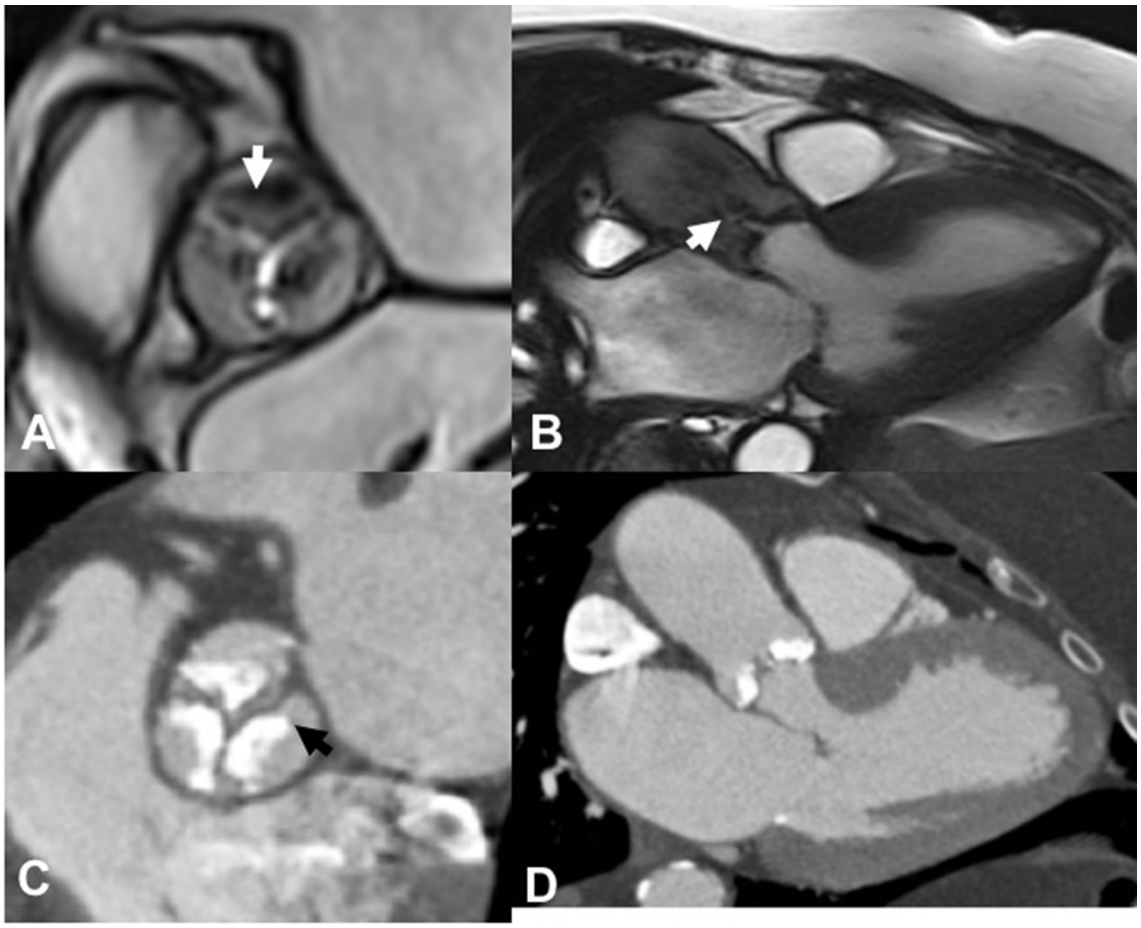

subvalvular stenosis[32] (Figure 3). On the other hand, PC-MRI enables to encoding the blood flow signal as velocity maps and to quantify functional parameters (*e.g.* flow, mean and peak velocity) and pressure gradient[37] (Figure 4).

Flow analysis performed by PC-MRI typically utilizes a monodirectional 2D ECG-triggered acquisition, able to quantify velocities in a single direction perpendicular to the acquired plane ("through-plane" velocity encoding orientation). However, this approach requires proper slice orientation that should be exactly perpendicular to the AS jet direction and located at the level of the opening of the valve orifice (not at the level passing through the valvular annulus), which commonly is the point of maximum flow acceleration, otherwise Vpeak is underestimated.[37] Therefore, an appropriate planning of the acquisition planes by the operator with respect to the valve leaflets and the stenotic jet is crucial for a precise flow velocity measurement, and it could be challenging in valvular abnormalities associated with multiple or eccentric jets.[38] Commonly, in the presence of severe AS, the markedly accelerated flow requires additional flow images after increasing Venc (from 200 to 500 cm s^{-1}) in order to avoid velocity aliasing artifacts. The recent improvements obtained with the 3D PC-MRI sequences (4D Flow) not only allow to orientate the three-dimensional geometric position of the sampling plan during post-processing, but also to adapt the plan orientation in each timeframe, as the jet direction may vary throughout the cardiac cycle.[38]

PC-MRI shows a high degree of correlation (Pearson's correlation coefficient from 0.61 to 0.81) regarding flow derived parameter (mean and peak velocity and gradient, AVA) with respect to TTE[38] and a good correlation with invasive pressure measurements.[37]

Software-assisted valve tracking algorithms offered by some vendors are promising to further improve the accuracy of flow measurement using 3D PC-MRI.

CMR is considered the gold-standard for studying LV function[39–41] and it showed a higher interstudy reproducibility than

Figure 3. CineMR images acquired on three-chamber (A, B) and on valve (C, D) views, and PC-MRI on valve plane. 46-years-old male with valvular stenosis (A, C, E) due to calcified commissure fusion with a raphe (triangle), where the flow-accelerated artifact is eccentric (arrow) and generated at the valve plane; the commissure makes the valve functionally bicuspid with the "fish mouth" opening on PC-MRI (E). 22-years-old female with sub-valvular stenosis (B, D, F) caused by a congenital diaphragm anchored to the septum: the artifact originates at the level of obstruction (arrow); although the valve has a normal tricuspid morphology (D) and a "fish mouth" shape of valve flow (F) reflecting the eccentricity of upstream stenosis. PC-MRI, phase contrast MRI.

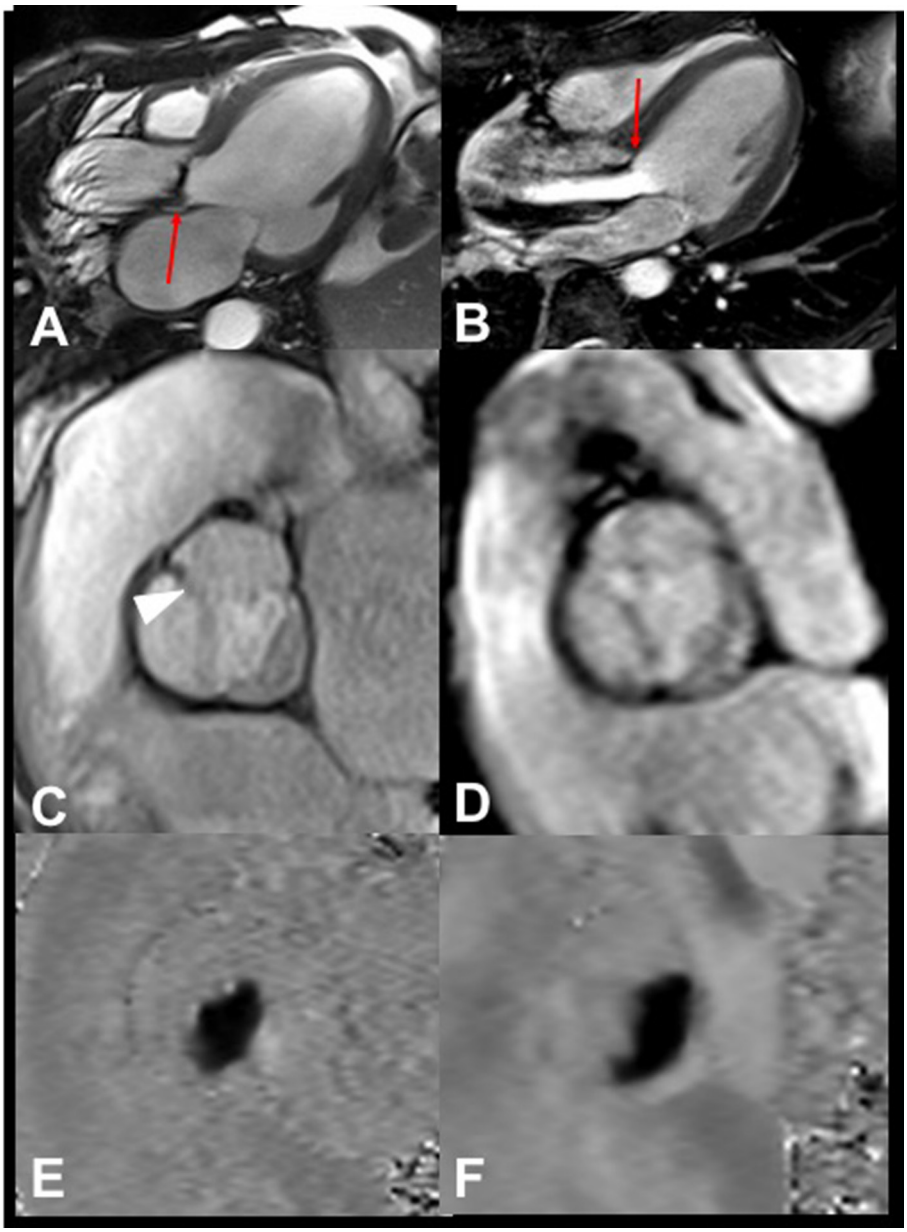

echocardiography for LV mass (2.8–4.8% *vs* 11.6–15.7%, $p < 0.001$), LV ejection fraction (LVEF)(2.4 – 7.3% *vs* 8.6 – 19.4%, $p < 0.001$) and LV end-systolic volume (4.4–9.2% *vs* 13.720.3%; $p < 0.001$).[42] Additionally, the assessment of myocardial strain by CMR feature tracking, beyond traditional functional parameters, allows an accurate analysis of the myocardial deformation,[43] resulting in a earlier and more sensitive recognition of LV contractile dysfunction with respect to LVEF.[44]

Furthermore, in considering the valve defect and the AS-related ascending aortopathy as a single "aortic stenosis complex",[45] CMR has the potential to merge morphological and functional valve features with the aortic anatomy and flow hemodynamics,[46] the latter by using 4D Flow imaging, which also enables the identification of regions of ascending aorta with increased wall shear stress.[47,48]

CMR has the unique capability to evaluate in a "all-in-one technique" all the principal severity parameters of AS (valve anatomy, valve hemodynamics, aortic and LV remodelling) and is able to provide pre-repair assessment[49,50] and prognostic information[10,51,52] (see specific sections).

Figure 4. MRI images from a 65-year-old male with severe aortic stenosis. Cine-MR images "on valve plane" shows a tricuspid aortic valve with a marked reduction of leaflet opening in systole (A). Aortic valvular area is measured on PC-MRI (B) by contouring the luminal edge of leaflets (red contour) and was severely reduced (0.85 mm2). On cineMR images acquired three chamber (C) and left outflow (D) views valve stenosis appears as a systolic jet of blood acceleration (flow void artifact) on downstream flow (arrows). The velocimetric study of aortic valve conducted by PC-MRI (E) demonstrates a high peak systolic velocity at the center of the valve orifice (light turquoise on the colorimetric map, Vpeak: 360 cm s–1), which indirectly represents an elevated gradient across the valve, with no regurgitation on the valve flow curve (F). PC-MRI, phase contrast MRI.

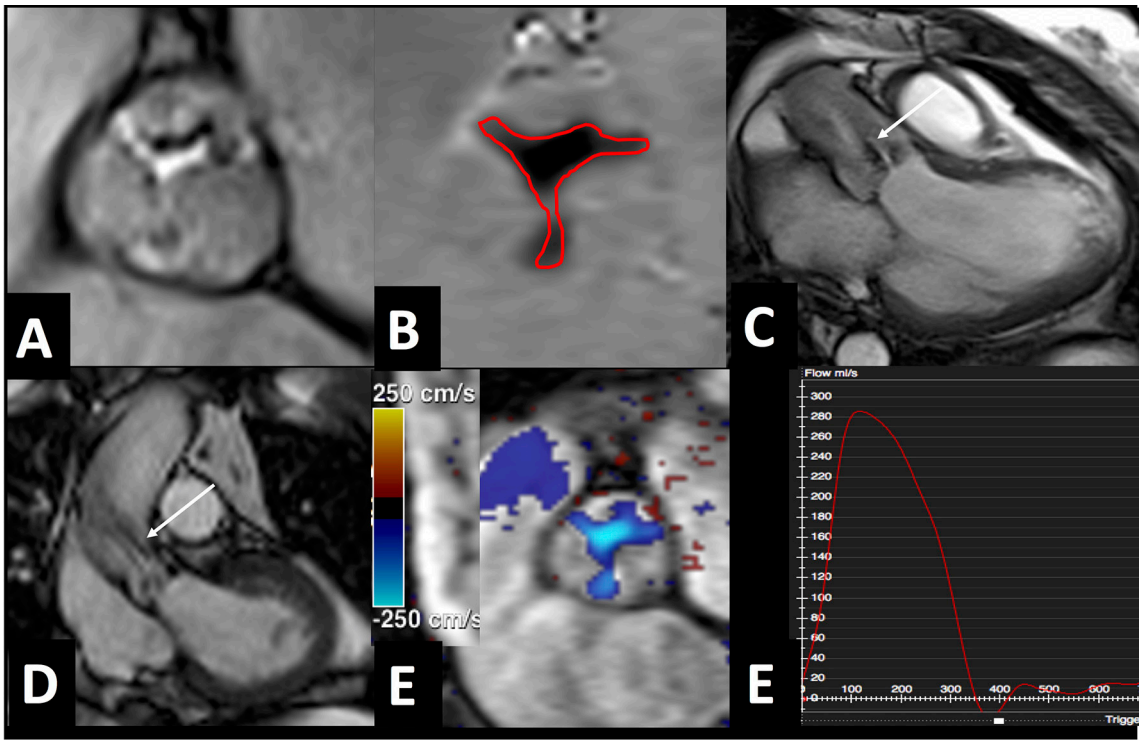

Aortic valve regurgitation

Aortic regurgitation (AR) is defined as the diastolic reflux of blood from the aorta to the LV, caused by the malcoaptation of the aortic leaflets. This condition may depend on primary impairment of valve leaflets, by an alteration of aortic root morphology, or both.[53]

Similar to the scheme used for AS, AR can be classified into different stages, based on valve morphology, valve hemodynamics, severity of LV dilation, LV systolic function, and symptoms: stage A includes patients at risk of AR, stage B patients with progressive mild-to-moderate AR, stage C severe asymptomatic AR, and stage D symptomatic AR[4,5]

Correct clinical grading is pivotal to prevent and predict morbidity and mortality, with prognosis ranging from excellent, in asymptomatic patients with normal LV function,[54] to poor in subjects with moderate to severe disease.[55]

CMR may offer both qualitative and quantitative analysis of AR and LV response to volume overload. AR severity can be approximately assessed on cineMR images using long axis LVOT views, where it is represented by the typical signal void of the regurgitation jet, backflowing into the ventricular lumen during diastole, which in some cases may impact on the anterior leaflet of the mitral valve, preventing its correct opening and exacerbating the diastolic dysfunction. Visually, a wide jet at the origin on the valve plane suggests more severe regurgitation. However, this technique is prone to many potential errors and the size of the jet may be not necessarily correlated to the severity of insufficiency, since it is caused by the local acceleration of the flow and does not directly reflect the regurgitant volume (RGV).

When precise or serial assessment of RGV is needed, CMR can accurately quantify the amount of regurgitation using flow mapping and derived values such as regurgitant fraction (RF = RGV/forward volume×100%) can be obtained.[56]

Flow characteristics can be assessed by acquiring the PC-MRI slice and quantifying both forward and regurgitant flows per cardiac cycle.[56]

PC-MRI plane should be positioned just below the valve, otherwise an underestimation of the regurgitation can occur due to a number of factors, including through-plane motion of the valve plane,[56] even though a more reproducible estimation of AR is obtained with a plane positioned at the sino-tubular junction. Indeed, PC-MRI technique is accurate and robust when the regurgitant flow is laminar and the jet is exactly perpendicular to the imaging planes. In some cases, the excessive motion of the valve plane may interfere with the RGV measurement;

acquisition of multiple PC-MRI planes at different levels may increase accuracy.

PC-MRI demonstrated a high precision and reproducibility of RGV measurement both *in vitro* and *in vivo*[57–60] and correlates well with the degrees of severity assessed by TEE and ICA.[60–62]

CMR may also measure the anatomic regurgitant orifice (ARO) by manually contouring the internal edge of valve leaflets in systole. In particular, Debl et al found a strong correlation of ARO with RGV and RF as assessed by CMR ($p < 0{,}001$) and with invasively evaluated AR at catheterization ($p = 0{,}01$).[63] Based on CMR parameter AR may be classified into mild (RF <20%), moderate (RF: 20–29%, ARO: 0.3–0.5 cm^2) and severe (RF ≥30%, ARO ≥ 0.5 cm^2), when PC-MRI images are acquired at the sino-tubular junction.[64] However, there is no unanimous consensus about the optimal threshold for classifying severe AR by CMR, as other studies demonstrated that a value above 33% strongly predicted the need of surgery in 3 years, similarly to the value of 50% used in echocardiography.[28,65]

Severe AR is also considered severe in case of reduced LV function parameters (LVEF <50 %, LV end-diastolic dimension ≤70 mm, LV end-systolic dimension ≤50 mm, and indexed LV end-systolic dimension <25 mm/m).[2,4] Compared to linear measurements, LV volumes measured by CMR seems to better predict survival and outcome.[65] Assessment of LV end-diastolic and end-systolic volumes indexed for body surface area should be obtained serially,[64] because even in asymptomatic patients with normal LV function, LV progressive dilatation is a reasonable indication for surgery.[4] Considering the importance of annual follow-up in patients with mild to severe AR, in order to estimate the progression of the disease, it is important not to classify chronic regurgitation as severe only on the basis of a single TTE or CMR.

CMR is a robust technique in providing accurate and reproducible assessment of regurgitation and LV response overtime, which is crucial to manage this condition characterized by a long asymptomatic phase and to guide the optimal timing of surgery.

Mixed aortic valve disease (MAVD)

MAVD is defined as the coexistence of both aortic regurgitation and aortic stenosis, at least of moderate degree of severity[66] (Figure 5). From a pathophysiological point of view, in MAVD the ventricle must adapt to accommodate both an elevated afterload and an increased stroke volume, resulting in a more pronounced LV remodelling.[67] Zilberszac et al[66] demonstrated that aortic valve jet velocity was the single most important independent predicting factor for event-free survival. In addition, LV mass and prevalence of advanced diastolic dysfunction were higher in

Figure 5. CMR images from a 66-year-old male with mix stenotic-regurgitant valvular disease. Cine-MR (A, D) and PC-MRI (B, E) images acquired "on valve plane" show a tricuspid aortic valve with reduced opening in systole (A, B) and small defect of coaptation (D, E) on diastole. Valvular flow is codified as black when anterograde (B) and white when backward (E) on PC-MRI. The regurgitant diastolic volume is calculated as the area under the curve of the backward flow on the flow curve (C). Cine-MR on three chamber view (F) depicts the impact of the regurgitating diastolic jet on the anterior leaflet of mitral valve, hindering the valve opening and accentuating diastolic dysfunction. CMR, cardiovascular magnetic resonance; PC-MRI, phase contrast MRI.

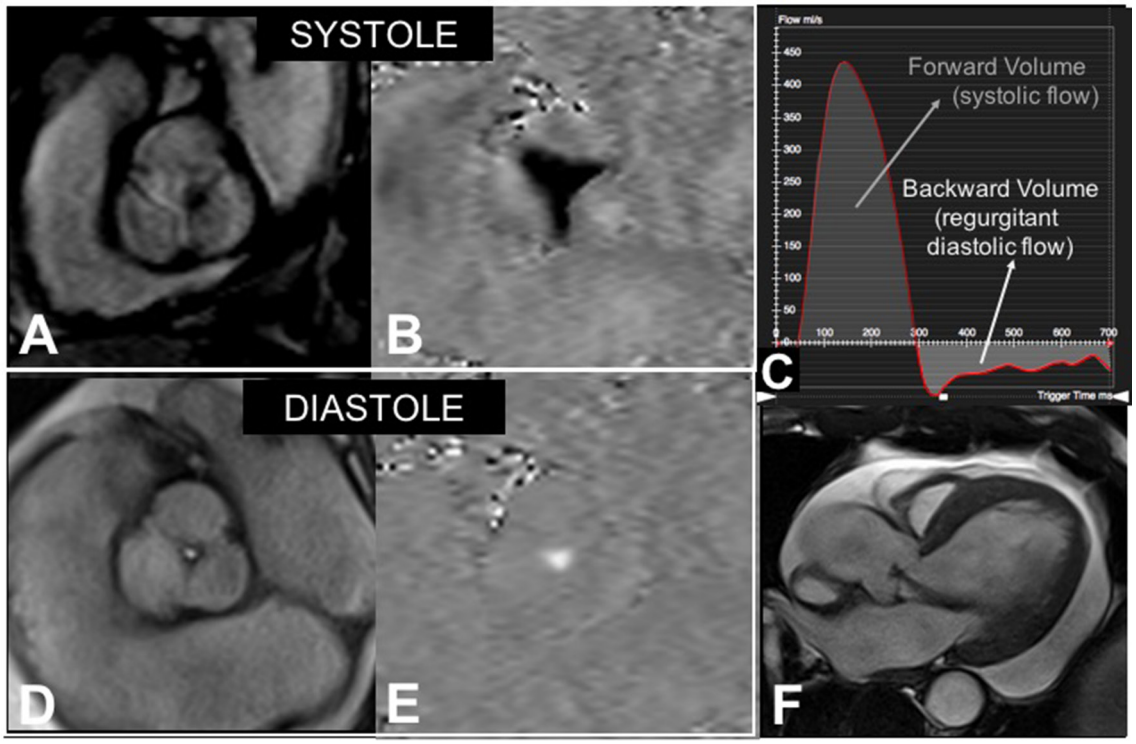

patients with MAVD with respect to moderate AR, moderate AS and severe AS (138 *vs* 94 g m^{-2} *vs* 103*v s* 123 g m^{-2}, $p < 0.02$ and 32 *vs* 5% *vs* 12 *vs* 22%, $p < 0.03$, respectively).[68] Only a few studies have been designed to specifically address the role of CMR in MAVD, even though it can provide an accurate and independent evaluation of the different component of the disease.[56] A modification of PC-MRI is recommended for MAVD assessment. Indeed, two axial planes are required on the LVOT, the first just below the aortic valve for measuring aortic regurgitation and the second at the tip of valve leaflets to quantify peak velocity.[69] In addition, while diastolic dysfunction appeared to be the main alteration leading to the onset of symptoms,[67] CMR myocardial strain analysis could be an additional tool for early recognition of ventricular contractile impairment.

PRE-PROCEDURAL PLANNING

Before surgical aortic valve repair (SAVR)

SAVR is indicated in low-risk patients with severe AS (class D), in AR patients with stages C2 and D or with class C/D undergoing cardiac surgery for other reasons.[4] The choice between bioprosthetic or mechanical valves depends on patient's age and life expectancy; in particular, mechanical valves have greater durability (20–30 years) than the bioprosthetic ones (10–15 years) but they require lifelong anticoagulation therapy.[70]

The role of CMR in SAVR planning is growing since it allows to precisely assess the size of the aortic root, valve morphology, the associated aortic abnormalities, surgical access and relationships of aortic root with the surrounding structures. In addition, the LV evaluation offered by CMR allows a more accurate estimate of the degree of hypertrophy, LV function and myocardial viability, which is particularly useful for potential candidates of a SAVR and coronary bypass combined procedure. A more important role of CMR in the selection of patients for valve replacement would be helpful for recognizing those who would benefit from AVD correction, even in terms of clinical outcome and LV reverse remodelling.[10,71]

However, in clinical practise, the use of CMR in pre-surgical planning is still marginal in many centers, a secondary choice compared to echocardiogram and CTA, generally limited to selected cases (young patients or those with renal failure).

Before TAVI

TAVI is a minimally invasive alternative to conventional SAVR based on the transcatheter deployment of specific bioprosthetic valves using a transaortic, transfemoral or transapical approach.

The procedure has shown to improve quality of life and to prolong short- and mid-term survival of high risk individuals (non-eligible for SAVR), becoming a widely accepted therapeutic option which has been integrated in the most recent clinical guidelines for management of AVD.[4,5]

TAVI is specifically recommended for patients with severe AS (class D) and a high surgical risk (STS score >8–10% or EuroSCORE II > 15–20%).[4,5] More recently, the SURTAVI[6] and PARTNER 2 trials[7] showed that TAVI is comparable to surgery even among intermediate surgical risk individuals, with no statistically significant differences in death or disabling stroke risk at 24 months (respectively 12.6 *vs* 14.0% in SURTAVI trial and 19.1 *vs* 21.1% in PARTENER II trial, respectively). For these reasons, a steep increase in the number of TAVI procedures may soon be expected, accompanied by a rising demand of pre- and post-TAVI imaging examinations.[72]

Pre-TAVI imaging is routinely performed for planning the preffered anatomic access and selecting the type and the size of implanted prosthesis[73] (Figure 6).

CCTA is considered as gold-standard[73] because of its wide availability, ease of use and comprehensiveness, covering the whole spectrum of required anatomical information, from the evaluation of the annular and aortic root to imaging of the coronary arteries and peripheral vascular vessels.

However, TAVI candidates, may be ineligible to CCTA in up to 20% of cases due to the presence of coexisting borderline renal function, in the context of which the use of an additional iodine dose (preceding the intervention) should be avoided to reduce the cumulative risk of acute kidney injury.[74]

In such cases, CMR may be a valid alternative to CCTA[49,73] using non-contrast enhanced techniques, like the 3D-SSFP ECG-gated navigator-echo (so-called "whole heart") for thoracic aorta and the various available flow-enhanced or flow-independent based MR angiography sequences for the evaluation of the aorto-iliac arteries.[72,75,76]

Anatomical region	*Detailed info*
Thoracic	Aortic valve morphology, LV geometry, annular size, aortic root measurement, coronary arteries height, aortic root angulation, and ascending aorta dimension.
Peripheral access	Superficial femoral arteries anatomy and guidewire/catheter pathway to the valve.

LV, left ventricular;

The method has shown an excellent correlation with CCTA for all the relevant pre-procedural parameters regarding aortic root including annulus size, aortic leaflet length, and coronary artery ostia height. It systemically underestimates the amount of leaflet calcifications which have been demonstrated to be a negative predictor of post-procedural paravalvular leak, particularly when located in the so-called "landing zone" valvular area, where the prosthetic device is attached although calcium estimation is not a key parameter for selection.[76] An additional strength of CMR, is the excellent temporal resolution of the method which allows to obtain high quality motion-free images of the aortic root even in patients with higher heart rates, suggesting its possible utilisation in individuals that respond poorly to beta blockers[76]

On cross-sectional imaging, the shape of aortic root is circular at the level of the sino-tubular junction, but take a more clover-leaf shape at the level of the aortic sinus, often becoming oval to ellipsoid at the annular plane and the LVOT. In heavily calcified anatomy with

Figure 6. TAVI planning. Based on cineMR imaging of left ventricular outflow tract and aortic root (A) and three-chambers view (E). The precise measurements of the aortic root diameters are performed by acquiring a stack of axial plane cine images perpendicular to the longitudinal axis of the vessel at the sino-tubular junction (B), sinuses of Valsalva (C) and valve annulus (D) levels. Dedicated oblique cineMR plane are acquired in order to measure the distance between the coronary orifices and the valve plane (F left coronary artery, G right coronary artery, respectively). MR angiography of aorta and femoraliliac axes (H) is also performed to assess the vascular access of the introducer system. TAVI, transcatheter aortic valve implantation.

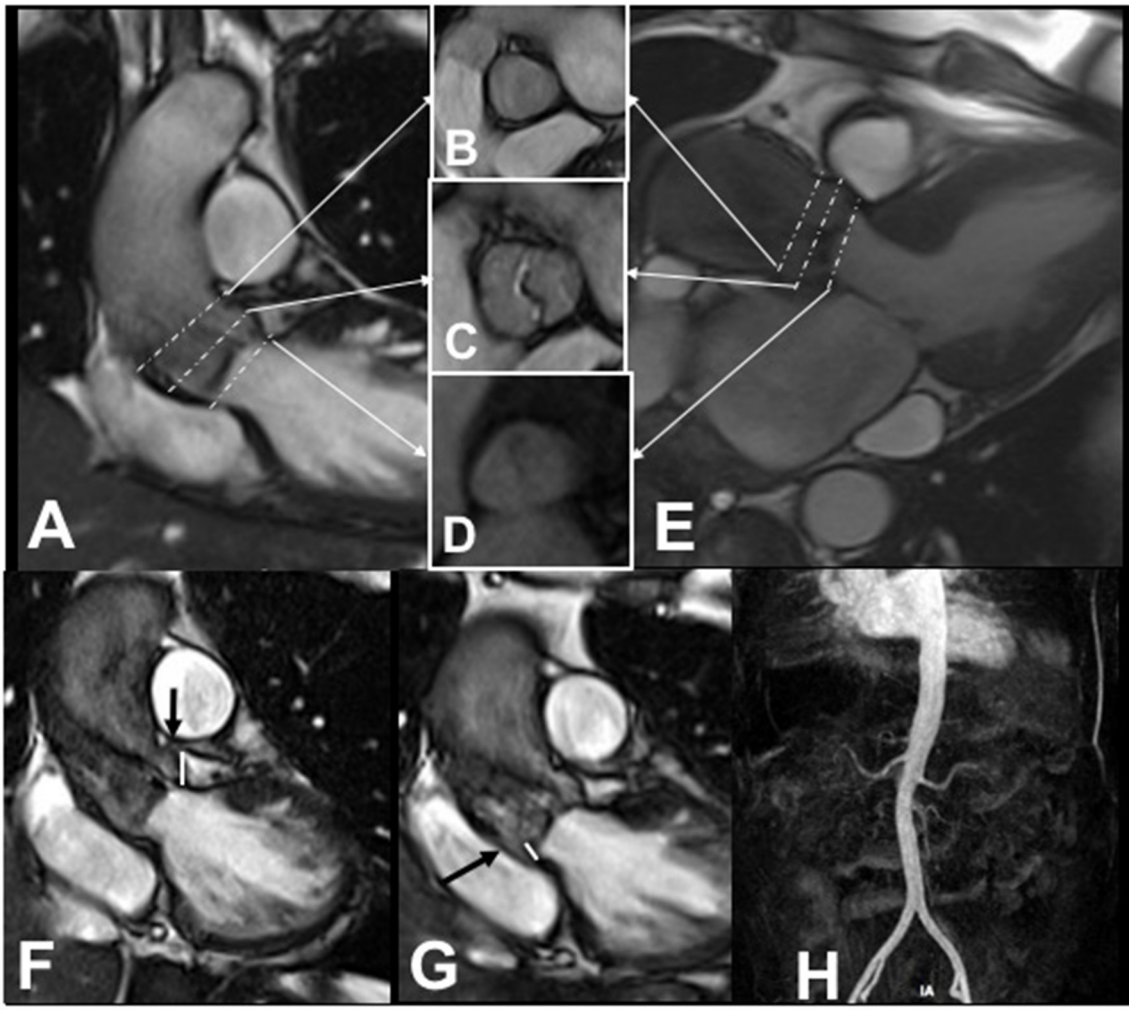

severe aortic stenosis/incompetence, the cross-sectional shape can be even more complex and not comparable to geometric assumptions. Precise measurements of aortic dimensions is crucial for procedural success, since a small differences in the choice of a measurement plane in the aortic root and choice of start–end point of the selected diameter can produce notably different results influencing the choice of endograft size. Therefore, high-quality images are essential in order to provide reliable measurements.

Finally, still favoring CMR utilization in pre-TAVI planning, is the incremental prognostic value of this method, which derives from its unique tissue characterization capabilities, making it suitable for postoperative outcome prediction (see dedicated paragraph).

POST-PROCEDURAL IMAGING

The sternal wire and the mechanical valve prostheses are generally MR compatible, yet the magnetic field inhomogeneities produced by the metal component of the devices (particularly for mechanical prostheses) may decrease image quality.[77] Therefore, the ability of CMR to detect and recognize valve complications depends on the type of implanted device. Biological prostheses include homografts, pulmonary autografts, and xenografts (stentless and stented), whose neo-leaflets are generally made of porcine heart valves or bovine pericardium and well assessed by CMR (Figure 7).[77] The assessment of AV is not recommended for mechanical prostheses (including those used in TAVI) due to the significant susceptibility artifacts caused by the prosthetic material, which prevent visualization of the valvular and paravalvular regions (Figure 7).[77]

Although TTE has an undisputed role in the post-SAVR follow-up, CMR could play a pivotal role in the evaluation of

Figure 7. CineMR images acquired on three chamber and LVOT views acquired in systolic (middle row) and diastolic (bottom row) phases of patients subject to valve replacement with mechanical (A, D, G) and biological prosthesis (B, E, H), and valve sparing aortic root replacement (C, F, I). Assessment of mechanic prosthesis is characterised by remarkable artifacts of magnetic susceptibility due to the high metallic content, which makes the function of prosthetic components poorly evaluable. The biological prosthesis has a peripheral metal ring with an absence of signal, whereas the leaflets are clearly assessable. Aortic surgery with valve sparing technique does not alter the visualization of the valve cusps. LVOT, left ventricular outflow tract.

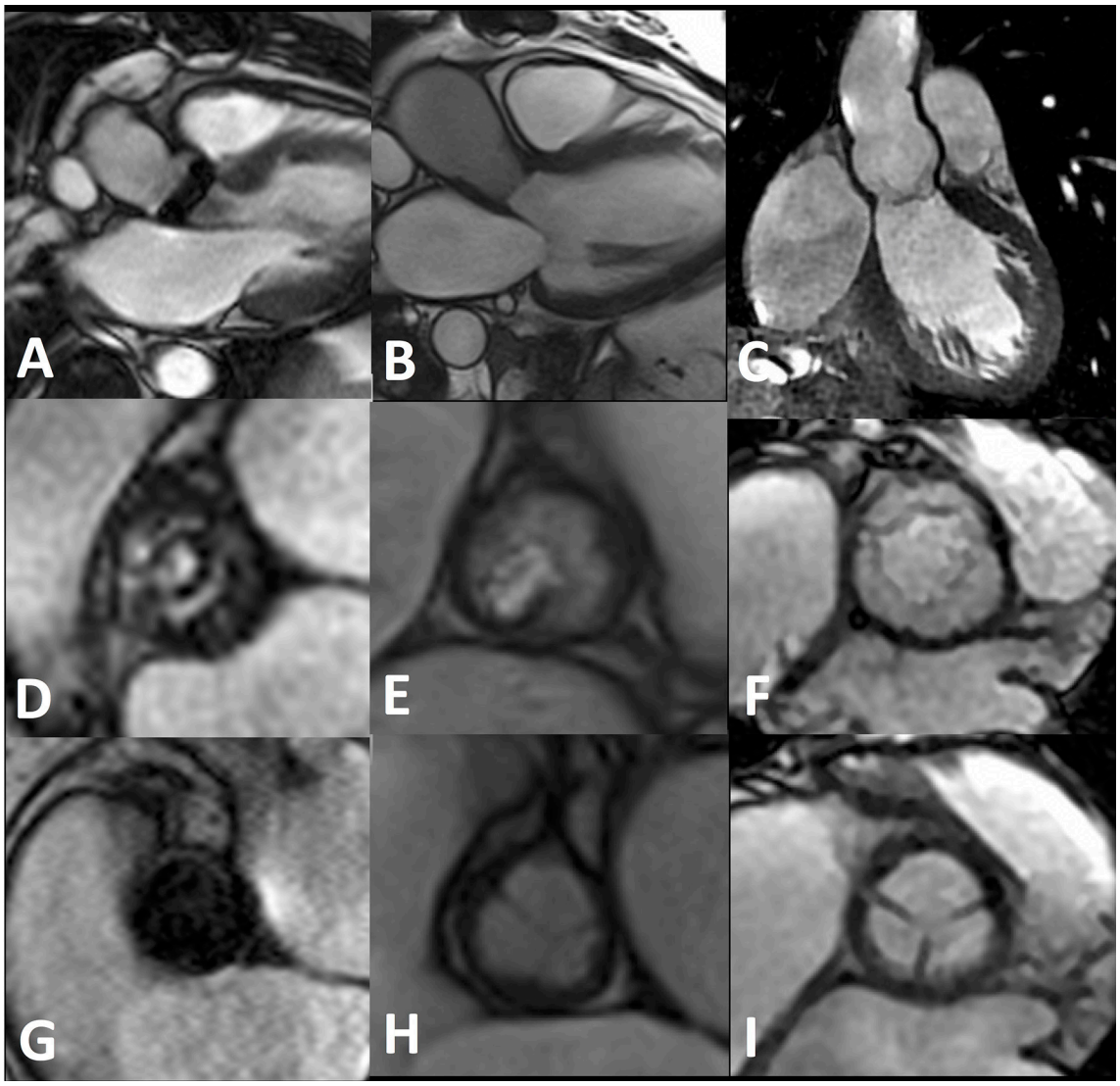

short- and long-term effects on valve function and ventricular remodelling, when an adequate image quality is obtained.

CineMR is particularly useful and accurate in quantifying the effective orifice area, which is essential to recognize prosthesis–patient mismatch, and to visualize the incomplete opening or closing of one or more of the prosthetic cusps, sometimes identifying the underlying cause (*e.g.* pannus ingrowth or thrombosis).[77]

As with native aortic valves, PC-MRI is able to measure transprosthetic blood flow velocities and is able to quantify peak transprosthetic velocity, tranvalvular gradient and transvalvular backflow in cases of residual or recurrent valve regurgitation.[77]

CMR may also accurately assess the LV reverse remodelling and the mass regression occuring immediately after SAVR, predictiving good long-term prognosis, or over time during follow-up.[78] Interestingly, recent evidence revealed a gender difference in AS-related hypertrophy (males are associated with greater degree of hypertrophy) and on remodeling response (more pronounced in females).[79]

CMR plays also a role in the detection and follow-up of SAVR complications, including paravalvular leakage (PVL), dehiscence, obstruction, structural failure, aortic dissection, pseudoaneurysm formation (Figure 8), endocarditis and hemolysis.[80] Apart from hemolysis, CMR is able to characterize all these potential adverse events.

Figure 8. Cine-MR images acquired on outflow tract plane (A) and valve planes (B) from a 26-year-old male with a history of surgical replacement of aortic valve with a mechanic prosthesis who developed a subvalvular pseudoaneurism (*) from suture dehiscence (arrow), extending in proximity of the atrioventricular junction and the right coronary ostium.

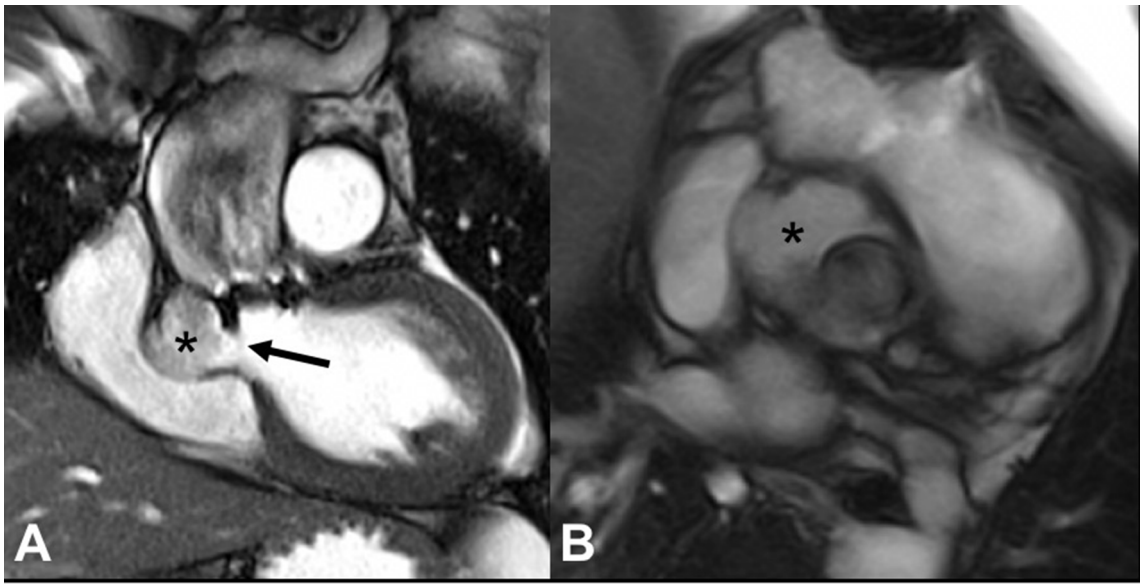

PVL refers to regurgitation between the prosthetic sewing ring and the surrounding anchoring tissue and is a serious SAVR complication.[81] Paradoxically, a minimal PVL is desired and required to aid device closure during diastole.[81] However, PVL can reveal dehiscence and malposition of the valve. At CMR imaging, PVL appears as a dephasing artifact in the three chamber view and can be quantified using the PC-MRI, with a plane positioned just below the valve.[82] The PARTNER trial found out that paravalvular leak was more frequent in TAVI than in SAVR (6.8% *vs* 1.9%),[83] although in other studies paravalvular regurgitation in SAVR occurred in 10 to 48% of patients.[78]

Dehiscence is the spontaneous breakdown of the surgical sutures sewed between the prosthetic valve and the annulus and it may represent a life threatening condition. Its leading cause is infective endocarditis, usually extending into nearby soft tissues.[84] The most common CMR findings include the presence of PVL and of a gap between the prosthetic valve and the annulus, using the cine-MR sequences through an "on annulus" plane.[80]

The implanted valve can be obstructed by thrombosis (prevalence 0.3–1%) and pannus formation (incidence 0.2–4.5% patients/years).[80] The differential diagnosis cannot be performed with the echocardiographic imaging modalities (TOE and TTE);[85] conversely, CT attenuation is able to differentiate a thrombus (hypodense structure adhering to the prosthesis) from a pannus (its attenuation should be similar to that of the ventricular septum).[80] Although only a few CMR studies have addressed this issue, its intrinsic ability of tissue characterization may add crucial information on implanted valve obstruction.

The prevalence of bioprosthetic valve structural failure ranges from 30% for heterograft valves to 10–20% for homograft valves within 10–15 years, whereas the incidence of this complication for mechanical valves is only 0.01–0.05% per patient/year.[80]

Stanford type A aortic dissection occurs in approximately 0.6% of post-SAVR patients[86] but it appears to be more related to the intrinsic aortic wall abnormalities (aortic wall fragility, aortic regurgitation, and aortic wall thinning) rather than to the surgical procedure itself.[80] According to Nienaber et al,[87] MRI showed 100% sensitivity, specificity, accuracy, positive predictive value and negative predictive value.

Pseudoaneurysm formation is 27 times more common in composite graft (7–25% of the patients), where the aortic root is replaced by an mechanical or biological valve pre-mounted on an tube graft, with respect to aortic valve replacement alone.[88] In case of clinical suspicion, a prompt TTE evaluation is mandatory. CMR is helpful in the differential diagnosis between pseudoaneurysm and other pathological diverticular lesions and for assessing the patency of coronary ostia.[80]

Emerging applications of CMR include the investigation of the relationship between specific surgical techniques and resulting aortic hemodynamics, which could help to customize the intervention to the individual anatomy.[89]

VALVULAR MASSES AND PSEUDOMASSES

Aortic valvular masses are uncommon and include benign and malignant disease and pseudomasses like vegetations (Figure 9), paravalvular abscesses (Figure 10) and pseudoaneurysms (Figure 8).

Neoplastic heart disease is rare, with a prevalence ranging from 0.0017 to 0.33.[90] Secondary involvement from a cardiac disease is 20–40 times more frequent than primary malignant lesion.[90–92] However, cardiac neoplasms are mostly benign (75% of cases).[90,91] Papillary fibroelastoma is the most common cause of aortic valve tumor, accounting for 10% of the benign cardiac tumors. Other neoplasms may involve the

Figure 9. CMR from a 67-year-old male with an aortic valve vegetation, secondary to endocarditis. CineMR "on valve plane" (A) and outflow tract plane images (B) show a hypointense vegetation attached to the aortic side of the non-coronary valve leaflet (white arrow).

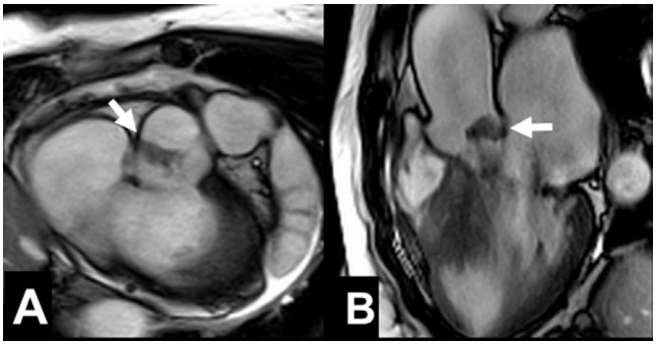

aortic valvular apparatus such as myxoma, hamartoma, lipoma, metastasis.[90,93]

Generally, the first imaging of choice in the diagnosis and characterization of valvular masses is echocardiography. However, despite its technical limitations, CMR may help to further evaluate valvular masses. The sequences used to assess the valve are indicated in the Expert Consensus Document on CMR,[94] and they would include cine-MR sequence on the plane of the valve to assess mass mobility and 3D SSFP with a T_2 preparatory pulse and fat suppression on the plane of the valve, to improve spatial resolution.

CMR may be helpful in distinguishing benign from malignant neoplasms, as shown by Hoffman et al. (area under receiver operator curve 0.90).[95] CMR can easily evaluate important features, such as location, tissue inhomogeneity, infiltration of adjacent compartments, tumor size, presence of pericardial or pleural effusion, and contrast enhancement[96] An important limitation of CMR compared to CCTA is the inability to study calcifications of cardiac masses. Nonetheless, it gives important information about myocardial abnormalities and allows imaging in multiple planes and providing information about functional impairment.

Figure 10. CMR and CCTA from a 58-year-old male with valve endocarditis complicated by paravalvular abscess. On Cine-MR "on valve plane" (A) and three-chamber (B) views the aortic valve appears diffusely thicked and narrowed. Paravalvular abscesses appear as little saccular collections localized between the sinuses of Valsalva (arrows), also detectable on the corresponding CCTA reformatted image(C). CCTA, coronary CT angiography; CMR, cardiovascular magnetic resonance.

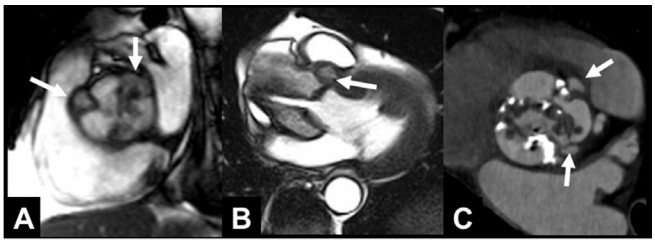

Moreover, CMR may be helpful in those challenging cases, when the risk of misdiagnosis caused by the sub optimal imaging quality at echocardiographic study, makes difficult to differentiate between vegetation and tumor.[97] Indeed, CMR performed better in the imaging evaluation of cardiac masses over a combination of TTE and TEE, discerning between masses and thrombi in 75% cases compared with 29% cases of echocardiography.[98] However, aortic endocarditis, despite being more common than aortic valve neoplasm, remains a sporadic disease (median incidence range of infective endocarditis from 1993 to 2003; 0.3–22.4%).[99]

Concerning other rare pseudolesions, such as pseudoaneurysms or valvular abscesses, CMR may be helpful in assessing the extent of the disease. Both pathologies are related to post-SAVR infection. Infective endocarditis may develop from a paravalvular abscess or a cavity contiguous with a cardiac chamber (pseudoaneurysm). CMR may aid to characterize their localization and extension; particularly, cine-MR may evaluate the presence of communication between the abscess cavity and the cardiac chambers. Finally, it is a non-invasive and accurate exam in the follow-up of patients with perivalvular extension of infection.

PROGNOSTIC IMPLICATION OF CMR: FIBROSIS EQUATES WITH PROGNOSIS

Myocardial fibrosis is an end-stage manifestation of aortic valvular pathology characterized by the accumulation of extracellular matrix proteins causing an expansion of the interstitial space, with subsequent impairment of the ventricular properties and progressive systo–diastolic dysfunction.[13] The process is known to be complex and multifactorial, depending on the equilibrium between myocyte growth and death, with an overexpression of profibrotic cytokines stimulating fibroblasts activation. In AVDs, fibrotic remodelling is triggered by the volume or pressure overload.

The model of AS has shown that tissue fibrosis occurs in a late stage of the disease, following the initial myocyte hypertrophy which triggers the activation of myocardial fibroblasts, leading to an inflammatory response that controls the turnover of collagen, with the development of both diffuse interstitial and focal replacement fibrosis.[100] In the AR disease tissue, fibrosis occurs during the initial phase of adaptive hypertrophy, in which more elastic forms of collagen are accumulated to maintain an adequate ventricular compliance being gradually replaced, in late stages, by inelastic matrix causing progressive heart failure.[11,101]

Regardless of the underlying mechanisms, tissue fibrosis is a major prognostic determinant in AVD, causing a damage to the structural integrity of the heart, with loss of its electrical conductive properties.[13] These histologic changes in myocardial tissue are mostly irreversible and results in sub-optimal outcomes after valvular replacement.[102]

CMR is the gold-standard for non-invasive assessment of myocardial fibrosis, which can be detected directly with late-gadolinium

enhancement (LGE) and T1 mapping and indirectly with feature-tracking techniques. Furthermore, the multiparametricity of the CMR allows not only to detect the presence of fibrosis, but also to distinguish chronic from acute tissue damage, which is typically characterized by the occurrence of myocardial edema on T_2 weighted images.[103]

LGE may detect areas of replacement fibrosis, which represents the irreversible final stage of focal myocardial damage.[104] Azevedo et al[10] demonstrated a good correlation between fibrosis assessed with LGE and histopathology ($r = 0.69$, $p < 0.001$), and an inverse correlation between LV functional improvement after surgery and presence of LGE ($r = -0.47$; $p = 0.02$), with a worse long-term survival after AVR ($X^2 = 5.85$; $p = 0.02$).

Furthermore, LGE is predictive of increase in all-cause and cardiac mortality in patient with AS.[105]

Quantification of native T_1 mapping, has emerged as a novel alternative approach for the depiction of diffuse inflammatory processes, deriving from generation of parametric maps which allow the quantification of T_1 relaxation times in any region of the heart.

Diffuse myocardial infiltrative and reactive interstitial fibrosis are reliably detected by an increase of native myocardial T_1 value and expansion of extracellular volume fraction after gadolinium administration.[106]

Several studies have demonstrated the alteration of T_1 mapping values compared to control cases, in both aortic stenosis and regurgitation[10,107–109] because of the congestion of interstitial space by collagen type molecules in AS[110] and fibronectin/non-collagen molecules in AR.[111] Chin et al[108] found an increased ECV in patient with AS and mid-wall fibrosis compared to controls.

The greater rigidity and lesser contractility of altered myocardium occurring in diffuse fibrosis causes impaired myocardial strain, that can be assessed by CMR using feature tracking technique.

Recently, Al Musa et al[12] demonstrated that patients with severe AS had a significantly worsened longitudinal and circumferential strain values compared to controls, which also correlated with the postoperative functional recovery and clinical outcome.[71] Interestingly patients with severe AS and no or mild symptoms demonstrate a comparable reduction in circumferential and longitudinal strain to those with significant symptoms.[12]

Current guidelines recommend valvular replacement mainly for patient with symptomatic severe valvular disease, or LV function impairment. In future, tissue characterization offered by CMR could be helpful in patient stratification by identifying those asymptomatic patients with subclinical interstitial myocardial fibrosis that would benefit from an early treatment to prevent progression to symptomatic stage, heart failure and irreversible fibrosis.

CONCLUSION

The AVD is a complex group of different pathological entities requiring a multidisciplinary approach. From an imaging point of view, CMR is an all-in-one technique able to investigate all the different aspects of the disease, ranging from early diagnosis to prognostic evaluation and pre- and post-treatment assessment. Although the guidelines consider CMR as a second line tool, it is more reproducible than echocardiography concerning valve morphology, valve flow and ventricular function evaluation; furthermore, its unique ability to provide histologically *in vivo* information has a pivotal role in the detection of ventricular fibrosis and, therefore, in the prognostic patient stratification.

ACKNOWLEDGMENT

Authors gratefully acknowledge professor Guido Ligabue (Modena, Italy) for providing support for this paper in cases selection.

REFERENCES

1. Nkomo VT, Gardin JM, Skelton TN, Gottdiener JS, Scott CG, Enriquez-Sarano M. Burden of valvular heart diseases: a population-based study. *Lancet* 2006; **368**: 1005–11. doi: https://doi.org/10.1016/S0140-6736(06)69208-8
2. Iung B, Baron G, Butchart EG, Delahaye F, Gohlke-Bärwolf C, Levang OW, et al. A prospective survey of patients with valvular heart disease in Europe: The Euro Heart Survey on Valvular Heart Disease. *Eur Heart J* 2003; **24**: 1231–43. doi: https://doi.org/10.1016/S0195-668X(03)00201-X
3. Marquis-Gravel G, Redfors B, Leon MB, Généreux P. Medical treatment of aortic stenosis. *Circulation* 2016; **134**: 1766–84. doi: https://doi.org/10.1161/CIRCULATIONAHA.116.023997
4. NishimuraRA, OttoCM, BonowRO, CarabelloBA, ErwinJP, GuytonRA. AHA/ACC guideline for the management of patients with valvular heart disease. *Circulation* 2014; **2014**: CIR-0000000000000031.
5. Baumgartner H, Falk V, Bax JJ, De Bonis M, Hamm C, Holm PJ, et al. 2017 ESC/EACTS Guidelines for the management of valvular heart disease. *Eur Heart J* 2017; **38**: 2739–91. doi: https://doi.org/10.1093/eurheartj/ehx391
6. Reardon MJ, Van Mieghem NM, Popma JJ, Kleiman NS, Søndergaard L, Mumtaz M, et al. Surgical or Transcatheter Aortic-Valve Replacement in Intermediate-Risk Patients. *N Engl J Med* 2017; **376**: 1321–31. doi: https://doi.org/10.1056/NEJMoa1700456
7. Leon MB, Smith CR, Mack MJ, Makkar RR, Svensson LG, Kodali SK, et al. Transcatheter or surgical aortic-valve replacement in intermediate-risk patients. *N Engl J Med Overseas Ed* 2016; **374**: 1609–20. doi: https://doi.org/10.1056/NEJMoa1514616
8. Lee SC, Ko SM, Song MG, Shin JK, Chee HK, Hwang HK. Morphological assessment of the aortic valve using coronary computed

tomography angiography, cardiovascular magnetic resonance, and transthoracic echocardiography: comparison with intraoperative findings. *Int J Cardiovasc Imaging* 2012; **28**(Suppl 1): 33–44. doi: https://doi.org/10.1007/s10554-012-0066-9
9. Zoghbi WA, Adams D, Bonow RO, Enriquez-Sarano M, Foster E, Grayburn PA, et al. Recommendations for noninvasive evaluation of native valvular regurgitation: A report from the american society of echocardiography developed in collaboration with the society for cardiovascular magnetic resonance. *J Am Soc Echocardiogr* 2017; **30**: 303–71. doi: https://doi.org/10.1016/j.echo.2017.01.007
10. Azevedo CF, Nigri M, Higuchi ML, Pomerantzeff PM, Spina GS, Sampaio RO, et al. Prognostic significance of myocardial fibrosis quantification by histopathology and magnetic resonance imaging in patients with severe aortic valve disease. *J Am Coll Cardiol* 2010; **56**: 278–87. doi: https://doi.org/10.1016/j.jacc.2009.12.074
11. Barone-Rochette G, Piérard S, De Meester de Ravenstein C, Seldrum S, Melchior J, Maes F, et al. Prognostic significance of LGE by CMR in aortic stenosis patients undergoing valve replacement. *J Am Coll Cardiol* 2014; **64**: 144–54. doi: https://doi.org/10.1016/j.jacc.2014.02.612
12. Al Musa T, Uddin A, Swoboda PP, Garg P, Fairbairn TA, Dobson LE, et al. Myocardial strain and symptom severity in severe aortic stenosis: insights from cardiovascular magnetic resonance. *Quant Imaging Med Surg* 2017; **7**: 38–. doi: https://doi.org/10.21037/qims.2017.02.05
13. Ambale-Venkatesh B, Lima JA. Cardiac MRI: a central prognostic tool in myocardial fibrosis. *Nat Rev Cardiol* 2015; **12**. doi: https://doi.org/10.1038/nrcardio.2014.159
14. PiazzaN, de JaegereP, SchultzC, BeckerAE, SerruysPW, AndersonRH. Anatomy of the aorticvalvarcomplex and itsimplications for transcatheterimplantation of the aorticvalve. *CircCardiovascInterv* 2008; **1**: 74–81.
15. Katayama S, Umetani N, Sugiura S, Hisada T. The sinus of Valsalva relieves abnormal stress on aortic valve leaflets by facilitating smooth closure. *J Thorac Cardiovasc Surg* 2008; **136**: 1528–. doi: https://doi.org/10.1016/j.jtcvs.2008.05.054
16. Singh S, Ghayal P, Mathur A, Mysliwiec M, Lovoulos C, Solanki P. Unicuspid unicommissuralaorticvalve: anextremelyrarecongenitalanomaly. *Tex Heart InstJ* 2015; **42**: 273–6.
17. Looi JL, Kerr AJ, Gabriel R. Morphology of congenital and acquired aortic valve disease by cardiovascular magnetic resonance imaging. *Eur J Radiol* 2015; **84**: 2144–54. doi: https://doi.org/10.1016/j.ejrad.2015.07.022
18. Ward C. Clinical significance of the bicuspid aortic valve. *Heart* 2000; **83**: 81–5. doi: https://doi.org/10.1136/heart.83.1.81
19. Hiratzka LF, Bakris GL, Beckman JA, Bersin RM, Carr VF, Casey DE, et al. 2010 ACCF/AHA/AATS/ACR/ASA/SCA/SCAI/SIR/STS/SVM guidelines for the diagnosis and management of patients with Thoracic Aortic Disease: a report of the American College of Cardiology Foundation/American Heart Association Task Force on Practice Guidelines, American Association for Thoracic Surgery, American College of Radiology, American Stroke Association, Society of Cardiovascular Anesthesiologists, Society for Cardiovascular Angiography and Interventions, Society of Interventional Radiology, Society of Thoracic Surgeons, and Society for Vascular Medicine. *Circulation* 2010; **121**: e266–e369. doi: https://doi.org/10.1161/CIR.0b013e3181d4739e
20. Wassmuth R, von Knobelsdorff-Brenkenhoff F, Gruettner H, Utz W, Schulz-Menger J. Cardiac magnetic resonance imaging of congenital bicuspid aortic valves and associated aortic pathologies in adults. *Eur Heart J Cardiovasc Imaging* 2014; **15**: 673–9. doi: https://doi.org/10.1093/ehjci/jet275
21. Sabet HY, Edwards WD, Tazelaar HD, Daly RC. Congenitally bicuspid aortic valves: a surgical pathology study of 542 cases (1991 through 1996) and a literature review of 2,715 additional cases. *Mayo Clin Proc* 1999; **74**: 14–26. doi: https://doi.org/10.4065/74.1.14
22. Verma S, Siu SC. Aortic dilatation in patients with bicuspid aortic valve. *N Engl J Med Overseas Ed* 2014; **370**: 1920–9. doi: https://doi.org/10.1056/NEJMra1207059
23. Kwon MH, Sundt TM, ValvulopathyBA. Bicuspid aortic valvulopathy and associated aortopathy: a review of contemporary studies relevant to clinical decision-making. *Curr Treat Options Cardiovasc Med* 2017; **19**: 68. doi: https://doi.org/10.1007/s11936-017-0569-8
24. Piatti F, Sturla F, Bissell MM, Pirola S, Lombardi M, Nesteruk I, et al. 4D flow analysis of BAV-Related fluid-dynamic alterations: evidences of wall shear stress alterations in absence of clinically-relevant aortic anatomical remodeling. *Front Physiol* 2017; **8**: 441. doi: https://doi.org/10.3389/fphys.2017.00441
25. Tutarel O. The quadricuspid aortic valve: a comprehensive review. *J Heart Valve Dis* 2004; **13**: 534–7.
26. Braunwald's heart disease: a textbook of cardiovascular medicineTenth editioned Philadelphia, PAEl sevier/Saunders. 2015;.
27. CzarnyMJ, ResarJR. Diagnosis and management of valvularaorticstenosis. *ClinMed InsightsCardiol* 2014; **8**(Suppl 1): 15–24.
28. LeopoldJA. Cellular mechanisms of aorticvalvecalcification. *Circ CardiovascInterv* 2012; **5**: 605–14.
29. Paelinck BP, Van Herck PL, Rodrigus I, Claeys MJ, Laborde JC, Parizel PM, et al. Comparison of magnetic resonance imaging of aortic valve stenosis and aortic root to multimodality imaging for selection of transcatheter aortic valve implantation candidates. *Am J Cardiol* 2011; **108**: 92–8. doi: https://doi.org/10.1016/j.amjcard.2011.02.348
30. Senior R, Dwivedi G, Hayat S, Lim TK. Clinical benefits of contrast-enhanced echocardiography during rest and stress examinations. *Eur J Echocardiogr* 2005; **6**(Suppl 2): S6–S13.
31. Tanaka K, Makaryus AN, Wolff SD. Correlation of aortic valve area obtained by the velocity-encoded phase contrast continuity method to direct planimetry using cardiovascular magnetic resonance. *J Cardiovasc Magn Reson* 2007; **9**: 799–805. doi: https://doi.org/10.1080/10976640701545479
32. Cavalcante JL, Lalude OO, Schoenhagen P, Lerakis S. Cardiovascular Magnetic Resonance Imaging for Structural and Valvular Heart Disease Interventions. *JACC Cardiovasc Interv* 2016; **9**: 399–425. doi: https://doi.org/10.1016/j.jcin.2015.11.031
33. Garcia J, Marrufo OR, Rodriguez AO, Larose E, Pibarot P, Kadem L. Cardiovascular magnetic resonance evaluation of aortic stenosis severity using single plane measurement of effective orifice area. *J Cardiovasc Magn Reson* 2012; **14**: 23: 23: . doi: https://doi.org/10.1186/1532-429X-14-23
34. Kupfahl C, Honold M, Meinhardt G, Vogelsberg H, Wagner A, Mahrholdt H, et al. Evaluation of aortic stenosis by cardiovascular magnetic resonance imaging: comparison with established routine clinical techniques. *Heart* 2004; **90**: 893–901. doi: https://doi.org/10.1136/hrt.2003.022376
35. Mantini C, Di Giammarco G, Pizzicannella J, Gallina S, Ricci F, D'Ugo E, D'Ugo E, et al. Grading of aortic stenosis severity: a head-to-head comparison between cardiac magnetic resonance imaging and

echocardiography. *Radiol Med* 2018; **123**: 643–54. doi: https://doi.org/10.1007/s11547-018-0895-2
36. Glockner JF, Johnston DL, McGee KP. Evaluation of cardiac valvular disease with MR imaging: qualitative and quantitative techniques. *Radiographics* 2003; **23**: e9. doi: https://doi.org/10.1148/rg.e9
37. Nayak KS, Nielsen JF, Bernstein MA, Markl M, D Gatehouse P, M Botnar R, et al. Cardiovascular magnetic resonance phase contrast imaging. *J Cardiovasc Magn Reson* 2015; **17**: 71. doi: https://doi.org/10.1186/s12968-015-0172-7
38. da Silveira JS, Smyke M, Rich AV, Liu Y, Jin N, Scandling D, et al. Quantification of aortic stenosis diagnostic parameters: comparison of fast 3 direction and 1 direction phase contrast CMR and transthoracic echocardiography. *J Cardiovasc Magn Reson* 2017; **19**: 35. doi: https://doi.org/10.1186/s12968-017-0339-5
39. Keenan NG, Pennell DJ. CMR of ventricular function. *Echocardiography* 2007; **24**: 185–93. doi: https://doi.org/10.1111/j.1540-8175.2007.00375.x
40. Pennell DJ, ResonanceCM. Cardiovascular magnetic resonance. *Circulation* 2010; **121**: 692–705. doi: https://doi.org/10.1161/CIRCULATIONAHA.108.811547
41. Suinesiaputra A, Bluemke DA, Cowan BR, Friedrich MG, Kramer CM, Kwong R, et al. Quantification of LV function and mass by cardiovascular magnetic resonance: multi-center variability and consensus contours. *J Cardiovasc Magn Reson* 2015; **17**: 63. doi: https://doi.org/10.1186/s12968-015-0170-9
42. Grothues F, Smith GC, Moon JC, Bellenger NG, Collins P, Klein HU, et al. Comparison of interstudy reproducibility of cardiovascular magnetic resonance with two-dimensional echocardiography in normal subjects and in patients with heart failure or left ventricular hypertrophy. *Am J Cardiol* 2002; **90**: 29–34. doi: https://doi.org/10.1016/S0002-9149(02)02381-0
43. Andre F, Steen H, Matheis P, Westkott M, Breuninger K, Sander Y, et al. Age- and gender-related normal left ventricular deformation assessed by cardiovascular magnetic resonance feature tracking. *J Cardiovasc Magn Reson* 2015; **17**: 25. doi: https://doi.org/10.1186/s12968-015-0123-3
44. Schuster A, Hor KN, Kowallick JT, Beerbaum P, Kutty S. Cardiovascular magnetic resonance myocardial feature tracking: concepts and clinical applications. *Circ Cardiovasc Imaging* 2016; **9**: e004077. doi: https://doi.org/10.1161/CIRCIMAGING.115.004077
45. Boudoulas KD, Wolfe B, Ravi Y, Lilly S, Nagaraja HN, Sai-Sudhakar CB. The aortic stenosis complex: aortic valve, atherosclerosis, aortopathy. *J Cardiol* 2015; **65**: 377–82. doi: https://doi.org/10.1016/j.jjcc.2014.12.021
46. Girdauskas E, Rouman M, Disha K, Fey B, Dubslaff G, Theis B, et al. Functional aortic root parameters and expression of aortopathy in bicuspid versus tricuspid aortic valve stenosis. *J Am Coll Cardiol* 2016; **67**: 1786–96. doi: https://doi.org/10.1016/j.jacc.2016.02.015
47. Ha H, Kim GB, Kweon J, Lee SJ, Kim YH, Kim N, et al. The influence of the aortic valve angle on the hemodynamic features of the thoracic aorta. *Sci Rep* 2016; **6**: 32316. doi: https://doi.org/10.1038/srep32316
48. van Ooij P, Markl M, Collins JD, Carr JC, Rigsby C, Bonow RO, et al. Aortic valve stenosis alters expression of regional aortic wall shear stress: new insights from a 4-dimensional flow magnetic resonance imaging study of 571 subjects. *J Am Heart Assoc* 2017; **6**: e005959. doi: https://doi.org/10.1161/JAHA.117.005959
49. Rogers T, Waksman R. Role of CMR in TAVR. *JACC Cardiovasc Imaging* 2016; **9**: 593–602. doi: https://doi.org/10.1016/j.jcmg.2016.01.011
50. La Manna A, Sanfilippo A, Capodanno D, Salemi A, Polizzi G, Deste W, et al. Cardiovascular magnetic resonance for the assessment of patients undergoing transcatheter aortic valve implantation: a pilot study. *J Cardiovasc Magn Reson* 2011; **13**: 82: 82: . doi: https://doi.org/10.1186/1532-429X-13-82
51. Nigri M, Azevedo CF, Rochitte CE, Schraibman V, Tarasoutchi F, Pommerantzeff PM, et al. Contrast-enhanced magnetic resonance imaging identifies focal regions of intramyocardial fibrosis in patients with severe aortic valve disease: Correlation with quantitative histopathology. *Am Heart J* 2009; **157**: 361–8. doi: https://doi.org/10.1016/j.ahj.2008.09.012
52. Flett AS, Sado DM, Quarta G, Mirabel M, Pellerin D, Herrey AS, et al. Diffuse myocardial fibrosis in severe aortic stenosis: an equilibrium contrast cardiovascular magnetic resonance study. *Eur Heart J Cardiovasc Imaging* 2012; **13**: 819–26. doi: https://doi.org/10.1093/ehjci/jes102
53. Maurer G. Aortic regurgitation. *Heart* 2006; **92**: 994–1000. doi: https://doi.org/10.1136/hrt.2004.042614
54. Borer JS, Hochreiter C, Herrold EM, Supino P, Aschermann M, Wencker D, et al. Prediction of indications for valve replacement among asymptomatic or minimally symptomatic patients with chronic aortic regurgitation and normal left ventricular performance. *Circulation* 1998; **97**: 525–34. doi: https://doi.org/10.1161/01.CIR.97.6.525
55. Dujardin KS, Enriquez-Sarano M, Schaff HV, Bailey KR, Seward JB, Tajik AJ. Mortality and morbidity of aortic regurgitation in clinical practice. A long-term follow-up study. *Circulation* 1999; **99**: 1851–7.
56. Myerson SG. Heart valve disease: investigation by cardiovascular magnetic resonance. *J Cardiovasc Magn Reson* 2012; **14**: 7. doi: https://doi.org/10.1186/1532-429X-14-7
57. Chatzimavroudis GP, Oshinski JN, Franch RH, Walker PG, Yoganathan AP, Pettigrew RI. Evaluation of the precision of magnetic resonance phase velocity mapping for blood flow measurements. *J Cardiovasc Magn Reson* 2001; **3**: 11–19.
58. Dulce MC, Mostbeck GH, O'Sullivan M, Cheitlin M, Caputo GR, Higgins CB. Severity of aortic regurgitation: interstudy reproducibility of measurements with velocity-encoded cine MR imaging. *Radiology* 1992; **185**: 235–40. doi: https://doi.org/10.1148/radiology.185.1.1523315
59. CawleyPJ, Hamilton-CraigC, OwensDS, KriegerEV, StrugnellWE, MitsumoriL, et al. Prospective comparison of valveregurgitationquantitation by cardiacmagneticresonanceimaging and transthoracicechocardiography. *CircCardiovasc Imaging* 2013; **6**: 48–57.
60. Nayak KS, Nielsen JF, Bernstein MA, Markl M, D Gatehouse P, M Botnar R, et al. Cardiovascular magnetic resonance phase contrast imaging. *J Cardiovasc Magn Reson* 2015; **17**: 71. doi: https://doi.org/10.1186/s12968-015-0172-7
61. Chatzimavroudis GP, Oshinski JN, Franch RH, Walker PG, Yoganathan AP, Pettigrew RI. Evaluation of the precision of magnetic resonance phase velocity mapping for blood flow measurements. *J Cardiovasc Magn Reson* 2001; **3**: 11–19. doi: https://doi.org/10.1081/JCMR-100000142
62. Honda N, Machida K, Hashimoto M, Mamiya T, Takahashi T, Kamano T, et al. Aortic regurgitation: quantitation with MR imaging velocity mapping. *Radiology* 1993; **186**: 189–94. doi: https://doi.org/10.1148/radiology.186.1.8416562
63. Debl K, Djavidani B, Buchner S, Heinicke N, Fredersdorf S, Haimerl J, et al. Assessment of the anatomic regurgitant orifice in aortic regurgitation: a clinical magnetic resonance imaging study. *Heart*

2008; **94**: e8. doi: https://doi.org/10.1136/hrt.2006.108720
64. Nadeau-Routhier C, Marsit O, Beaudoin J. Current management of patients with severe aortic regurgitation. *Curr Treat Options Cardiovasc Med* 2017; **19**: 9. doi: https://doi.org/10.1007/s11936-017-0508-8
65. Myerson SG, d'Arcy J, Mohiaddin R, Greenwood JP, Karamitsos TD, Francis JM, et al. Aortic regurgitation quantification using cardiovascular magnetic resonance: association with clinical outcome. *Circulation* 2012; **126**: 1452–60. doi: https://doi.org/10.1161/CIRCULATIONAHA.111.083600
66. Zilberszac R, Gabriel H, Schemper M, Zahler D, Czerny M, Maurer G, et al. Outcome of combined stenotic and regurgitant aortic valve disease. *J Am Coll Cardiol* 2013; **61**: 1489–95. doi: https://doi.org/10.1016/j.jacc.2012.11.070
67. Parker MW, Aurigemma GP. The Simple Arithmetic of mixed aortic valve disease. *J Am Coll Cardiol* 2016; **67**: 2330–3. doi: https://doi.org/10.1016/j.jacc.2016.03.549
68. Egbe AC, Luis SA, Padang R, Warnes CA. Outcomes in moderate mixed aortic valve disease. *J Am Coll Cardiol* 2016; **67**: 2321–9. doi: https://doi.org/10.1016/j.jacc.2016.03.509
69. Masci PG, Dymarkowski S, Bogaert J. Valvular heart disease: what does cardiovascular MRI add? *Eur Radiol* 2008; **18**: 197–208. doi: https://doi.org/10.1007/s00330-007-0731-x
70. TillquistT, TillquistT, MaddoxT. Cardiac crossroads: deciding between mechanical or bioprosthetic heart valve replacement. *Patient Prefer Adherence* 2011; **91**: 91.
71. Musa TA, Uddin A, Swoboda PP, Fairbairn TA, Dobson LE, Singh A, et al. Cardiovascular magnetic resonance evaluation of symptomatic severe aortic stenosis: association of circumferential myocardial strain and mortality. *J Cardiovasc Magn Reson* 2017; **19**: 13. doi: https://doi.org/10.1186/s12968-017-0329-7
72. Jabbour A, Ismail TF, Moat N, Gulati A, Roussin I, Alpendurada F, et al. Multimodality imaging in transcatheter aortic valve implantation and post-procedural aortic regurgitation. *J Am Coll Cardiol* 2011; **58**: 2165–73. doi: https://doi.org/10.1016/j.jacc.2011.09.010
73. OttoCM, KumbhaniDJ, AlexanderKP, CalhoonJH, DesaiMY, KaulS, et al. 2017 ACC expert consensus decision pathway for transcatheter aortic valve replacement in the management of adults with aortic stenosis. *J Am Coll Cardiol* 2017; **69**: 1313–46.
74. Bagur R, Webb JG, Nietlispach F, Dumont E, De Larochellière R, Doyle D, et al. Acute kidney injury following transcatheter aortic valve implantation: predictive factors, prognostic value, and comparison with surgical aortic valve replacement. *Eur Heart J* 2010; **31**: 865–74. doi: https://doi.org/10.1093/eurheartj/ehp552
75. Gopal A, Grayburn PA, Mack M, Chacon I, Kim R, Montenegro D, et al. Noncontrast 3D CMR imaging for aortic valve annulus sizing in TAVR. *JACC Cardiovasc Imaging* 2015; **8**: 375–8. doi: https://doi.org/10.1016/j.jcmg.2014.11.011
76. Pontone G, Andreini D, Bartorelli AL, Bertella E, Mushtaq S, Gripari P, et al. Comparison of accuracy of aortic root annulus assessment with cardiac magnetic resonance versus echocardiography and multidetector computed tomography in patients referred for transcatheter aortic valve implantation. *Am J Cardiol* 2013; **112**: 1790–9. doi: https://doi.org/10.1016/j.amjcard.2013.07.050
77. von Knobelsdorff-Brenkenhoff F, Trauzeddel RF, Schulz-Menger J. Cardiovascular magnetic resonance in adults with previous cardiovascular surgery. *Eur Heart J Cardiovasc Imaging* 2014; **15**: 235–48. doi: https://doi.org/10.1093/ehjci/jet138
78. HahnRT, PibarotP, StewartWJ, WeissmanNJ, GopalakrishnanD, KeaneMG, et al. Comparison of transcatheter and surgical aortic valve replacement in severe aortic stenosis. *J Am Coll Cardiol* 2013; **61**: 2514–21.
79. Lee JM, Park SJ, Lee SP, Park E, Chang SA, Kim HK, et al. Gender difference in ventricular response to aortic stenosis: insight from cardiovascular magnetic resonance. *PLoS One* 2015; **10**: e0121684. doi: https://doi.org/10.1371/journal.pone.0121684
80. Pham N, Zaitoun H, Mohammed TL, DeLaPena-Almaguer E, Martinez F, Novaro GM, et al. Complications of aortic valve surgery: manifestations at CT and MR imaging. *Radiographics* 2012; **32**: 1873–92. doi: https://doi.org/10.1148/rg.327115735
81. Kliger C, Eiros R, Isasti G, Einhorn B, Jelnin V, Cohen H, et al. Review of surgical prosthetic paravalvular leaks: diagnosis and catheter-based closure. *Eur Heart J* 2013; **34**: 638–49. doi: https://doi.org/10.1093/eurheartj/ehs347
82. Pflaumer A, Schwaiger M, Hess J, Lange R, Stern H. Quantification of periprosthetic valve leakage with multiple regurgitation jets by magnetic resonance imaging. *Pediatr Cardiol* 2005; **26**: 593–4. doi: https://doi.org/10.1007/s00246-005-0821-y
83. Smith CR, Leon MB, Mack MJ, Miller DC, Moses JW, Svensson LG, et al. Transcatheter versus Surgical Aortic-Valve Replacement in High-Risk Patients. *N Engl J Med Overseas Ed* 2011; **364**: 2187–98. doi: https://doi.org/10.1056/NEJMoa1103510
84. Metz E, Hartmann M, von Birgelen C, Haalebos MM, Verhorst PM. Major dehiscence of infected aortic valve prosthesis with "rocking motion" but without diastolic paravalvular regurgitation. *Int J Cardiovasc Imaging* 2006; **22**: 771–4. doi: https://doi.org/10.1007/s10554-006-9106-7
85. Habets J, Symersky P, van Herwerden LA, de Mol BA, Spijkerboer AM, Mali WP, et al. Prosthetic heart valve assessment with multidetector-row CT: imaging characteristics of 91 valves in 83 patients. *Eur Radiol* 2011; **21**: 1390–6. doi: https://doi.org/10.1007/s00330-011-2068-8
86. von Kodolitsch Y, Loose R, Ostermeyer J, Aydin A, Koschyk DH, Haverich A, et al. Proximal aortic dissection late after aortic valve surgery: 119 cases of a distinct clinical entity. *Thorac Cardiovasc Surg* 2000; **48**: 342–6. doi: https://doi.org/10.1055/s-2000-8346
87. Nienaber CA, von Kodolitsch Y, Nicolas V, Siglow V, Piepho A, Brockhoff C, et al. The diagnosis of thoracic aortic dissection by noninvasive imaging procedures. *N Engl J Med* 1993; **328**: 1–9. doi: https://doi.org/10.1056/NEJM199301073280101
88. Enseleit F, Grünenfelder J, Braun J, Matthews F, Jenni R, van der Loo B. Formation of pseudoaneurysm after aortic valve replacement without previous endocarditis: a case-control study. *J Am Soc Echocardiogr* 2010; **23**: 741–6. doi: https://doi.org/10.1016/j.echo.2010.04.013
89. Galea N, Piatti F, Sturla F, Weinsaft JW, Lau C, Chirichilli I, et al. Novel insights by 4D Flow imaging on aortic flow physiology after valve-sparing root replacement with or without neosinuses. *Interact Cardiovasc Thorac Surg* 2018; **26**: 957–64. doi: https://doi.org/10.1093/icvts/ivx431
90. Silver Spring, MdIn*Tumors of the heart and great vessels*ARP Press2015
91. Grebenc ML, Rosado de Christenson ML, Burke AP, Green CE, Galvin JR, CardiacP. Primary cardiac and pericardial neoplasms: radiologic-pathologic correlation. *Radiographics* 2000; **20**: 1073–103. doi: https://doi.org/10.1148/radiographics.20.4.g00jl081073
92. Burke A, Tavora F, TheTF. The 2015 WHO Classification of Tumors of the Heart and Pericardium. *J Thorac Oncol* 2016; **11**: 441–52. doi: https://doi.org/10.1016/j.jtho.2015.11.009

93. Ghadimi MahaniM, LuJC, RigsbyCK, KrishnamurthyR, DorfmanAL, AgarwalPP. MRI of pediatriccardiacmasses. *AJRAmJRoentgenol* 2014; **202**: 971–81.
94. American College of Cardiology Foundation Task Force on Expert Consensus Documents, Hundley WG, Bluemke DA, Finn JP, Flamm SD, Fogel MA, et al. ACCF/ACR/AHA/NASCI/SCMR 2010 expert consensus document on cardiovascular magnetic resonance: a report of the American College of Cardiology Foundation Task Force on Expert Consensus Documents. *J Am Coll Cardiol* 2010; **55**: 2614–62. doi: https://doi.org/10.1016/j.jacc.2009.11.011
95. Hoffmann U, Globits S, Schima W, Loewe C, Puig S, Oberhuber G, et al. Usefulness of magnetic resonance imaging of cardiac and paracardiac masses. *Am J Cardiol* 2003; **92**: 890–5. doi: https://doi.org/10.1016/S0002-9149(03)00911-1
96. Lopez-Mattei JC, Shah DJ. The role of cardiac magnetic resonance in valvular heart disease. *Methodist Debakey Cardiovasc J* 2013; **9**: 142–8. doi: https://doi.org/10.14797/mdcj-9-3-142
97. Sommer T, Vahlhaus C, Hofer U, von Smekal A, Wardelmann E, Bierhoff E, et al. MRI diagnosis of cardiac myxomas: sequence evaluation and differential diagnosis. *Rofo* 1999; **170**: 156–62. doi: https://doi.org/10.1055/s-2007-1011028
98. Gulati G, Sharma S, Kothari SS, Juneja R, Saxena A, Talwar KK. Comparison of echo and MRI in the imaging evaluation of intracardiac masses. *Cardiovasc Intervent Radiol* 2004; **27**: 459–69. doi: https://doi.org/10.1007/s00270-004-0123-4
99. Moreillon P, Que YA. Infective endocarditis. *Lancet* 2004; **363**: 139–49. doi: https://doi.org/10.1016/S0140-6736(03)15266-X
100. Khan R, Sheppard R. Fibrosis in heart disease: understanding the role of transforming growth factor-beta in cardiomyopathy, valvular disease and arrhythmia. *Immunology* 2006; **118**: 10–24. doi: https://doi.org/10.1111/j.1365-2567.2006.02336.x
101. Liu SK, Magid NR, Fox PR, Goldfine SM, Borer JS, FibrosisBJS. Fibrosis, myocyte degeneration and heart failure in chronic experimental aortic regurgitation. *Cardiology* 1998; **90**: 101–9. doi: https://doi.org/10.1159/000006827
102. Weidemann F, Herrmann S, Störk S, Niemann M, Frantz S, Lange V, et al. Impact of myocardial fibrosis in patients with symptomatic severe aortic stenosis. *Circulation* 2009; **120**: 577–84. doi: https://doi.org/10.1161/CIRCULATIONAHA.108.847772
103. Francone M, Carbone I, Agati L, Bucciarelli Ducci C, Mangia M, Iacucci I, et al. Utility of T2-weighted short-tau inversion recovery (STIR) sequences in cardiac MRI: an overview of clinical applications in ischaemic and non-ischaemic heart disease. *Radiol Med* 2011; **116**: 32–46. doi: https://doi.org/10.1007/s11547-010-0594-0
104. Esposito A, Francone M, Faletti R, Centonze M, Cademartiri F, Carbone I, et al. Lights and shadows of cardiac magnetic resonance imaging in acute myocarditis. *Insights Imaging* 2016; **7**: 99–110. doi: https://doi.org/10.1007/s13244-015-0444-7
105. Dweck MR, Joshi S, Murigu T, Alpendurada F, Jabbour A, Melina G, et al. Midwall fibrosis is an independent predictor of mortality in patients with aortic stenosis. *J Am Coll Cardiol* 2011; **58**: 1271–9. doi: https://doi.org/10.1016/j.jacc.2011.03.064
106. Podlesnikar T, Delgado V, Bax JJ. Cardiovascular magnetic resonance imaging to assess myocardial fibrosis in valvular heart disease. *Int J Cardiovasc Imaging* 2018; **34**: 97-112. doi: https://doi.org/10.1007/s10554-017-1195-y
107. Lee SP, Lee W, Lee JM, Park EA, Kim HK, Kim YJ, et al. Assessment of diffuse myocardial fibrosis by using MR imaging in asymptomatic patients with aortic stenosis. *Radiology* 2015; **274**: 359–69. doi: https://doi.org/10.1148/radiol.14141120
108. ChinCW, EverettRJ, KwiecinskiJ, VeseyAT, YeungE, EssonG, et al. Myocardial Fibrosis and Cardiac Decompensation in Aortic Stenosis. *JACC Cardiovascular imaging* 2016;.
109. Sparrow P, Messroghli DR, Reid S, Ridgway JP, Bainbridge G, Sivananthan MU. Myocardial T1 mapping for detection of left ventricular myocardial fibrosis in chronic aortic regurgitation: pilot study. *AJR Am J Roentgenol* 2006; **187**: W630–W635. doi: https://doi.org/10.2214/AJR.05.1264
110. Hein S, Arnon E, Kostin S, Schönburg M, Elsässer A, Polyakova V, et al. Progression from compensated hypertrophy to failure in the pressure-overloaded human heart. *Circulation* 2003; **107**: 984–91. doi: https://doi.org/10.1161/01.CIR.0000051865.66123.B7
111. Borer JS, Truter S, Herrold EM, Falcone DJ, Pena M, Carter JN, et al. Myocardial fibrosis in chronic aortic regurgitation. *Circulation* 2002; **105**: 1837–42. doi: https://doi.org/10.1161/01.CIR.0000014419.71706.85
112. da Silveira JS, Smyke M, Rich AV, Liu Y, Jin N, Scandling D, et al. Quantification of aortic stenosis diagnostic parameters: comparison of fast 3 direction and 1 direction phase contrast CMR and transthoracic echocardiography. *J Cardiovasc Magn Reson* 2017; **19**: 35. doi: https://doi.org/10.1186/s12968-017-0339-5
113. Egbe AC, Poterucha JT, Warnes CA. Mixed aortic valve disease: midterm outcome and predictors of adverse events. *Eur Heart J* 2016; **37**: 2671–8. doi: https://doi.org/10.1093/eurheartj/ehw079
114. Rashedi N, Popović ZB, Stewart WJ, Marwick T. Outcomes of asymptomatic adults with combined aortic stenosis and regurgitation. *J Am Soc Echocardiogr* 2014; **27**: 829–37. doi: https://doi.org/10.1016/j.echo.2014.04.013
115. Salgado RA, Leipsic JA, Shivalkar B, Ardies L, Van Herck PL, Op de Beeck BJ, et al. Preprocedural CT evaluation of transcatheter aortic valve replacement: what the radiologist needs to know. *Radiographics* 2014; **34**: 1491–514. doi: https://doi.org/10.1148/rg.346125076
116. Chiang YP, Chikwe J, Moskowitz AJ, Itagaki S, Adams DH, Egorova NN. Survival and long-term outcomes following bioprosthetic vs mechanical aortic valve replacement in patients aged 50 to 69 years. *JAMA* 2014; **312**: 1323. doi: https://doi.org/10.1001/jama.2014.12679
117. Musa TA, Plein S, Greenwood JP. The role of cardiovascular magnetic resonance in the assessment of severe aortic stenosis and in post-procedural evaluation following transcatheter aortic valve implantation and surgical aortic valve replacement. *Quant Imaging Med Surg* 2016; **6**: 259–73. doi: https://doi.org/10.21037/qims.2016.06.05